مجلة جامعة بني وليد للعلوم الإنسانية والتطبيقية
تصدر عن جامعة بني وليد – ليبيا
Website: https://jhas-bwu.com/index.php/bwjhas/index
المجلد التاسع، العدد الثالث الصفحات (199-213) 2024م

التصميم الحاسوبي، الالتحام الجزيئي، تحليل تشابه الدواء، التنبؤ بنتيجة النشاط الحيوي وتقييمها النشاط المخدر لبعض نظائر الكيتامين الجديدة كمثبطات لـ pLGICs

محمد إبراهيم الشنباري ، سالم علي ابراهيم عتيق ، هيفاء محمد ميلاد بيترو
[3.2.1] قسم المختبرات ، كلية التقنية الطبية، جامعة الجفارة، ليبيا.
alshenbarymohammed@gmail.com

In Silico Design, Molecular Docking, Drug-likeness Analysis, Bioactivity Score Prediction and Evaluation Anesthetic Activity of Some Novel Ketamine Analogues as pLGICs Inhibitors

Mohammed Ibrahim Alshenbary[1], Salim Ali Ibrahim Ateeg [2], Haifa Mohamed Milad Bitrou [3]
[1.2.3] Department of Laboratories, College of Medical Technology, Al-Jaffara University, Libya.

تاريخ الاستلام:22-07-2024 تاريخ القبول: 11-08-2024 تاريخ النشر: 03-09-2024

الملخص:

تهدف هذه الورقة إلى دراسة محاكاة الالتحام الجزيئي لأيزومرات الكيتامين ، حيث تم إجراء محاكاة الالتحام الجزيئي لأيزومرات الكيتامين S &R و (22) مركبا من نظائرها ، كل من هذه المركبات يحتوي على اثنين من (S & enantiomers R)، للتنبؤ بطاقات الربط وثوابت التثبيط ، مستهدفا مستقبلات القنوات الأيونية ذات البوابات الخماسية (pLGICs) لتقييم نشاط التخدير. تم تنزيل التركيب البلوري للأشعة السينية لمستقبلات pLGICs للبروتين المستهدف من موقع بنك بيانات البروتين (PDB) ، بالرمز (f8h4). تم استخدام برنامج Discovery Studio Visualizer لإعداد ملفات بتنسيق PDB للجزيئات المصممة. تم إجراء تفاعلات الالتحام الجزيئي بين سلسلة A من البروتين المستهدف والروابط باستخدام برنامج AutoDockTools v.1.5.6.

وأشارت النتائج إلى أن (12) من أيزومرات (S) – للجزيئات المصممة ، (3 ، 4 ، 5 ، 7 ، 8 ، 9 ، 12 ، 18 ، 19 ، 20 ، 21 و 22) و (4) من (R) – أيزومرات (12 و 20 و 21 و 22) لها طاقات ربط أقل من الروابط القياسية (S) – الكيتامين (JC9) و (R) – الكيتامين (RKE) ومن المتوقع أن يكون لها تقارب كبير لمستقبلات pLGICs. علاوة على ذلك ، أظهرت نتائج التشابه مع الدواء باستخدام خادم ADME السويسري عبر الإنترنت أن جميع الجزيئات المصممة لديها توافر بيولوجي جيد ، 0.55 وتطيع قاعدة الخمسة (RO5) ، مع 0 انتهاك. نتائج نقاط النشاط الحيوي باستخدام شبكة Molinspiration. أظهر الخادم أن جميع الجزيئات لديها أنشطة جيدة لمعدل القناة الأيونية مع درجات نشاط حيوي من 0.02 إلى 0.86 ، باستثناء الجزيئات S11 و R11 ، والتي تنشط بشكل معتدل مع درجة النشاط الحيوي –0.04. استنتجت الدراسة

أن هذه المركبات تتوسط أنشطتها المخدرة عن طريق تنظيم القنوات الأيونية في الجهاز العصبي المركزي وأن جرعات أقل من هذه المركبات مطلوبة للتوسط في أنشطتها المخدرة.

الكلمات الدالة: الكيتامين ، التخدير ، في السيليكو ، الالتحام الجزيئي ، القناة الأيونية ذات البوابات الخماسية (pLGIC) ، التشابه الدوائي ، قاعدة Lipinski ، التوافر البيولوجي الفموي ، درجة النشاط الحيوي.

Abstract

This paper aims to study the simulation of molecular fusion of ketamine isomers, molecular docking simulation of S & R ketamine isomers and (22) compounds of its analogues, each of these compounds has two enantiomers (S & R), was performed to predict their binding energies and inhibition constants, targeting Pentameric Ligand-gated Ion Channels receptor (pLGICs) to evaluate the anesthetic activity. The X-ray crystallographic structure of the target protein pLGICs receptor was downloaded from Protein Data Bank (PDB) website, with the code (4f8h). Discovery Studio Visualizer software was used to prepare PDB format files of designed molecules. The molecular docking interactions between the A chain of target protein and the ligands were performed using AutoDockTools v.1.5.6 software. The results indicated that (12) of the (S)- isomers of the designed molecules, (**3, 4, 5, 7, 8, 9**, **12, 18, 19, 20, 21** and **22**) and (4) of the (R)-isomers (**12, 20, 21** and **22**) had lower binding energies than the standard ligands (S)-ketamine (**JC9**) and (R)-ketamine (**RKE**) and are predicted to have high affinities for pLGICs receptor. Furthermore, the drug-likeness results using the online Swiss ADME server showed that all of the designed molecules had good bioavailability, 0.55 and obeyed the Rule of five (RO5), with 0 violation. Bioactivity score results using Molinspiration web. server showed that all molecules had good ion channel modulator activities with bioactivity scores from 0.02 to 0.86, except molecules **11S and 11R**, which are moderately active with bioactivity score −0.04. It is concluded that these compounds mediate their anesthetic activities by regulating the ion channels in central nervous system and lower doses of these compounds are required to mediate their anesthetic activities.

Key words: ketamine, anesthesia, in silico, molecular docking, pentameric ligand gated ion channel (pLGIC), drug-likeness, Lipinski rule, oral bioavailability, bioactivity score.

1. Introduction

Ketamine is considered a general anesthetic drug, especially in children, prehospital and emergency department settings [1]. It is a phencyclidine derivative, synthesized by Calvin Stevens in the early 1962[2]. Figure 1 shows the two dimensional (2D) structures of ketamine and phencyclidine.

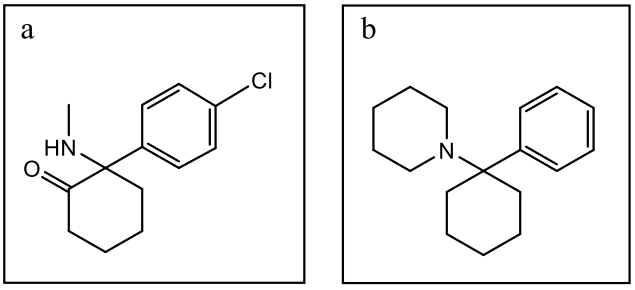

Figure 1: a) The 2D structure of ketamine. b) The 2D structure of phencyclidine

Phencyclidine was synthesized as a potent sedative agent in 1956. It was used clinically as a general anesthetic in 1963, but its use was prevented in the United States in 1965 because of its severe adverse effects including hallucination, blood hypertension and prolonged recovery from anesthesia [3,4]. In 1962 ketamine was developed as

a less hallucinogenic and shorter acting anesthetic agent [5]. Then it was introduced commercially in 1970 as rapidly acting general anesthesia[6]. Nowadays ketamine is not only a general anesthesia but also it presents a wide spectrum of pharmacological effects including hypnotic[7], analgesia[8], bronchodilation[9], anti-inflammatory[10], antihyperalgesia[11], anti-depressant [12], anti-epileptic[13] and protection against brain damage[14].

Ketamine, 2-(4-chlorophenyl)-2-(methylamino)cyclohexan-1-one contains a chiral center at the carbon-2 atom of the cyclohexanone ring, this leads to the presence of two optical isomers S(+) and R(-) ketamine with different pharmacological effects. The S-(+)-isomer is a fourfold more effective anesthesia than R-(-)-isomer and the use of S-(+)-isomer produces two-fold more activity and longer acting than the racemic mixture of both isomers. This means that half dose of S-(+) is needed as compared with the racemic ketamine [15]. Figure 2 shows the three dimensional (3D) structures of both ketamine enantiomers (S and R).

Ketamine performs their different pharmacological activities including anesthetic activity by interactions with numerous receptor systems in the human body including N-methyl-D-aspartate (NMDA) receptor and pLGICs receptor superfamily [16]. The human pLGICs receptor superfamily involves the Nicotinic acetylcholine receptors (nAChR), γ-aminobutyric acid (GABA) receptor, glycine- gated anion channels receptor (GlyR) and the 5-hydroxytryptamine type 3 (5-HT3) receptors [17].

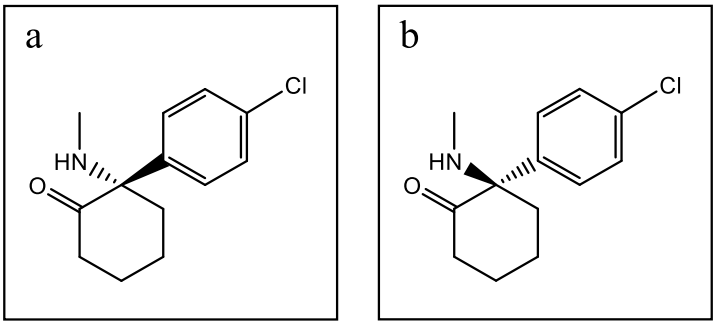

Figure 2: a) The 3D structure of (S)-ketamine isomer b) The 3D structure of (R)-ketamine isomer

As shown in figure 3 vertebrate pLGICs consist of five identical subunits that assemble forming channel pore. These channels are responsible for the fast signal transduction in central and peripheral nervous system [18]. Each subunit is composed of three domains, an extracellular or ligand-binding domain, a transmembrane domain forming channel pore, and an intracellular domain that maintains the direction of channel localization in the correct position in the nerve cell membrane and modulate effects of second messengers [19].

a) b)

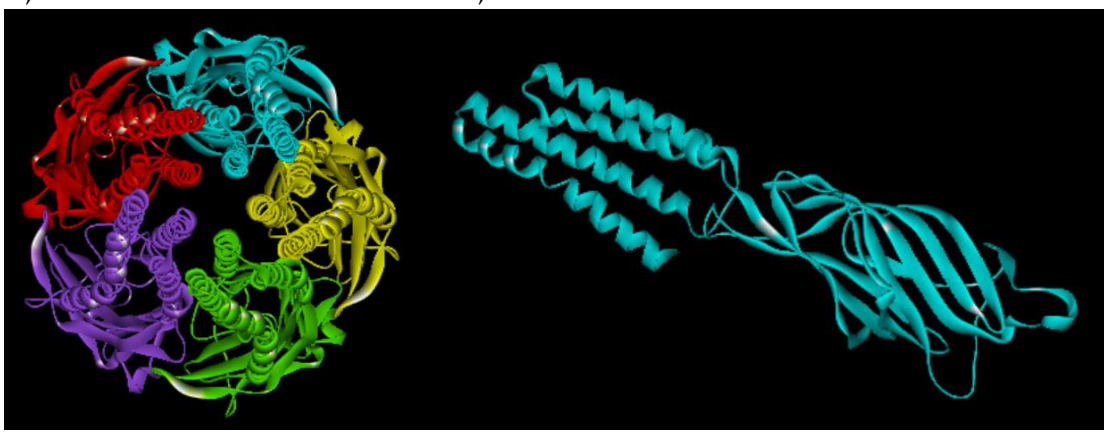

Figure 3: a) The 3D structure of pLGIC receptor b) The 3D structure of A chain of pLGIC receptor

The crystal structure of the bacterial pLGIC separated from *Gloeobacter violaceus* (GLIC) is structurally similar to vertebrate pLGICs [20], such as nicotinic acetyl choline receptors (nAChRs) except the intracellular domain, which is not essential for channel assembly and function [21]. General anesthetics such as ketamine can bind to extracellular domain of GLIC and in turn nAChRs subunit mediating reversible inhibition of the channel [22]. Molecular docking is a computational technique that be used in pharmaceutical research to predict the binding mode of a small molecule (ligand) to a specific protein receptor (target), by calculating the binding energy, which estimates the strength of binding between the ligand and target, mediating the biological activities [23].

2. Materials and Methods

The in-silico studies of molecular docking and drug likeness prediction, were performed using AutoDockTools (ADT) version 4.2[24], Discovery Studio Visualizer 2.5 (DS, Accelrys Software) [25], Cygwin64 terminal, free online Molinspiration and Swiss ADME servers [26]. All these softwares were run on a personal computer, HP with a processor of an Intel(R) Core(TM) i5-6300U CPU @ 2.40GHz 2.50 GHz and 1 TB (SSD) hard disk, generated with a random access memory (RAM) of 8 GB and windows 10 pro operating computer system.

2.1. Molecular docking studies

These included the preparation of receptor, standard S-ketamine, R-ketamine and designed compounds files required for docking procedure.

2.1.1. Receptor Preparation

The X-ray crystallographic structure of the target protein Pentameric Ligand-gated Ion Channels (pLGICs) receptor was downloaded from Protein Data Bank (PDB) website with the code (4f8h). The target receptor 4f8h was opened using Discovery Studio Visualizer software, water molecules were removed and all natural ligands were removed, followed by removing of chains B, C, D and E of the receptor and only chain A was kept as pdb file. Then polar hydrogen atoms were added and kollman charge was added to chain A by using AutoDockTools (ADT) 1.5.6 and the file was saved in pdbqt format.

2.1.2. Ligand preparation

The ideal 3D structures of S-ketamine (JC9) and R-ketamine (RKE) were downloaded from [Research Collaboratory for Structural Bioinformatics (RCSB)] web. Site. Chem Draw Professional 15.1 was used to draw the 2D structures of the designed ketamine analogues, which including 22S isomers and their 22R isomers. Figure 4 shows the 2D chemical structures of the designed compounds. Then the 2D structures were converted to PDB format using Discovery Studio Visualizer software.

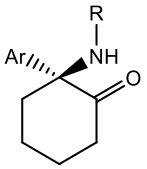

(S) isomers

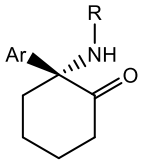

(R) isomers

Cpds	R	Ar	Cpds	R	Ar
1S	Me	2-fluorophenyl	**1R**	Me	2-fluorophenyl
2S	Me	2-bromophenyl	**2R**	Me	2-bromophenyl
3S	Me	2-hydroxyphenyl	**3R**	Me	2-hydroxyphenyl
4S	Me	2-nitrophenyl	**4R**	Me	2-nitrophenyl
5S	Me	2-methylphenyl	**5R**	Me	2-methylphenyl

6S	Me	3-chlorophenyl	**6R**	Me	3-chlorophenyl
7S	Et	2-chlorophenyl	**7R**	Et	2-chlorophenyl
8S	i-Pr	2-chlorophenyl	**8R**	i-Pr	2-chlorophenyl
9S	Me	4-chlorophenyl	**9R**	Me	4-chlorophenyl
10S	Me	4-bromophenyl	**10R**	Me	4-bromophenyl
11S	Et	2-bromophenyl	**11R**	Et	2-bromophenyl
12S	i-Pr	2-bromophenyl	**12R**	i-Pr	2-bromophenyl
13S	Et	2-hydroxyphenyl	**13R**	Et	2-hydroxyphenyl
14S	i-Pr	2-hydroxyphenyl	**14R**	i-Pr	2-hydroxyphenyl
15S	Et	2-nitrophenyl	**15R**	Et	2-nitrophenyl
16S	i-Pr	2-nitrophenyl	**16R**	i-Pr	2-nitrophenyl
17S	Me	2-chloropyridn-3-yl	**17R**	Me	2-chloropyridn-3-yl
18S	Me	2-bromopyridn-3-yl	**18R**	Me	2-bromopyridn-3-yl
19S	Me	2-aminophenyl	**19R**	Me	2-aminophenyl
20S	Et	2-aminophenyl	**20R**	Et	2-aminophenyl
21S	i-pro	2-aminophenyl	**21R**	i-pro	2-aminophenyl
22S	Me	2-aminophenyl-4-chloro	**22R**	Me	2-aminophenyl-4-chloro

Cpds-Compounds

Figure 4: The 3D structure of the designed molecules

In the next step the Gasteiger charges were added, nonpolar hydrogen atoms were emerged, all rotatable bonds made rotatable and the file was kept in pdbqt format by using AutoDockTools (ADT) 1.5.6.

2.1.3. Molecular docking

The molecular docking interactions between the A chain of protein target and the ligands were performed using AutoDockTools v.1.5.6 software to predict the binding energies, inhibition constants and the active binding site of the target protein pLGIC. The grid box in the x, y and z-dimensions were 60×60×60 points centered on a ligand with grid spacing of 0.375Å. All docking calculations for rigid protein and flexible ligands were made with the Lamarckian genetic algorithm (LGA) to search for the lowest binding energy. A population size of 150 and 2,500,000 energy evaluations was used for 50 search runs.

All docking parameters such as rate of gene mutation and rate of the crossover were set as default. After LGA run for each ligand, Auto dock reported the best docking solution for each docked complex, and the results were reported based on cluster analysis[27]. The binding energies of ligands to the target protein pLGIC were calculated with the help of Cygwin64 Terminal. The conformations with lowest docked energy were chosen, visualized and analyzed by Discovery Studio Visualizer.

2.2. Drug-likeness studies

The physicochemical properties and drug-likeness for (S)-ketamine, (R)-ketamine and all the designed molecules were theoretically calculated using the online SwissADME web. server. The 2D structures of the ligands were drawn on the server then automatically converted to Simplified Molecular-Input Line-Entry System (SMILES)

format. The predicted physicochemical properties, molecular weight, number of hydrogen bond donor (HBD), number of hydrogen bond acceptor (HBA), number of rotatable bonds (nRotB), total polar surface area (TPSA), molar refractivity (MR), MLogP- (Partitioning coefficient calculated by the Moriguchi I. et al.)[28], WlogP (Partitioning coefficient calculated by the Wildman et al.)[29] of the designed molecules were evaluated according to Lipinski's "rule of five"[30], Ghose, Veber [31]and Egan rules[32].

2.3. Bioactivity score prediction Molinspiration web. server was used to calculate the predicted bioactivity score for all the designed molecules against main human receptors, G-protein coupled receptor (GPCR), ion channels, kinase enzymes, nuclear receptors, protease enzymes and other enzymes.

3. Results and discussion

3.1 Docking Study

The (44) designed molecules were docked in the active site of A chain of pLGICs receptor using the same parameters applied in the docking study of standard ligand (S)-ketamine, and the predicted binding energies and inhibition constants resulted were listed in table 1.

Table 1: The binding energy and inhibition constants of S-ketamine, R-ketamine and the designed compounds.

Cpds	Binding energy Kcal/mol	Inhibition constant KI	Cpds	Binding energy Kcal/mol	Inhibition constant KI
1S	-3.3	3.79 mM	**1R**	-3.27	3.99 mM
2S	-4.16	891.2 □M	**2R**	-4.18	868.8 □M
3S	-5.58	80.7 □M	**3R**	-3.93	1.32 mM
4S	-5.41	108.7 □M	**4R**	-2.4	17.32 mM
5S	-4.32	675.99□□M	**5R**	-2.53	13.98 mM
6S	-4.05	1.08 mM	**6R**	0.42	Unavailable
7S	-5.73	63.61□□M	**7R**	0.66	Unavailable
8S	-6.25	26.28 □M	**8R**	0.68	Unavailable
9S	-5.72	64.07 □M	**9R**	0.37	Unavailable
10S	-3.74	1.82 mM	**10R**	0.41	Unavailable
11S	-1.13	147.44 mM	**11R**	-2.2	24,59 mM
12S	-4.6	424.43 □M	**12R**	-4.51	493.8 □M
13S	-1.66	60.91 mM	**13R**	-2.29	20.91 mM
14S	-1.71	55.88 mM	**14R**	-3.8	1.63 mM
15S	0.95	Unavailable	**15R**	-3.96	1.25 mM
16S	0.96	Unavailable	**16R**	-3.06	5.67 mM
17S	0.49	Unavailable	**17R**	-3.92	1.34 mM
18S	-5.55	85.31 □M	**18R**	-3.98	1.21 mM
19S	-6.43	19.35 □M	**19R**	-3.08	5.52 mM
20S	-5.46	99.01 □M	**20R**	-6.27	25.23 □M
21S	-5.52	89.54 □M	**21R**	-6.54	16.03 □M
22S	-6.23	27.11 □M	**22R**	-6.6	14.64 □M
JC9	-3.61	2.28 mM	**RKE**	-4.21	825.17□M

The active site of protein receptor that binds with (S)-ketamine was constituted by following amino acids residues: Thr-65, Tyr-66, Glu-67, Pro-68, Val-89, Val-90, Asp-91, Ile-92 and Ser-93. From the table 1, and based on the comparison of docking energy and inhibition constants, (12) of the (S)- isomers of the designed molecules, (**3, 4, 5, 7, 8, 9, 12, 18, 19,20, 21** and **22**) and (4) of the (R)-isomers (**12, 20, 21** and **22**) are predicted to have high affinities for pLGICs receptor and form more stable ligand-target complex, because they have lower binding energies with the active site of pLGICs receptor than the standard ligands (S)-ketamine (**JC9**) and (R)-ketamine (**RKE**). The best binding mode of (S)-ketamine to the pLGIC receptor is shown in figure 5, and for (R)-ketamine is shown in figure 6.

a) b) c)

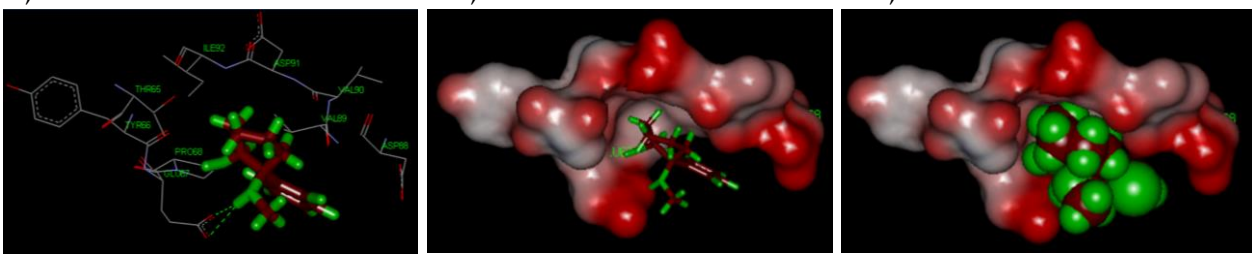

Figure 5: The best binding mode of **JC9** with the pLGICs receptor. a) The H-bond interactions formed by **JC9** and pLGIC. b) The docked pose of 3D structure (stick model) of **JC9** in pLGIC pocket. c) The docked pose of 3D CPK conformation of **JC9** in pLGIC pocket. (CPK-Corey-Pauling-Koltun model)

a) b) c)

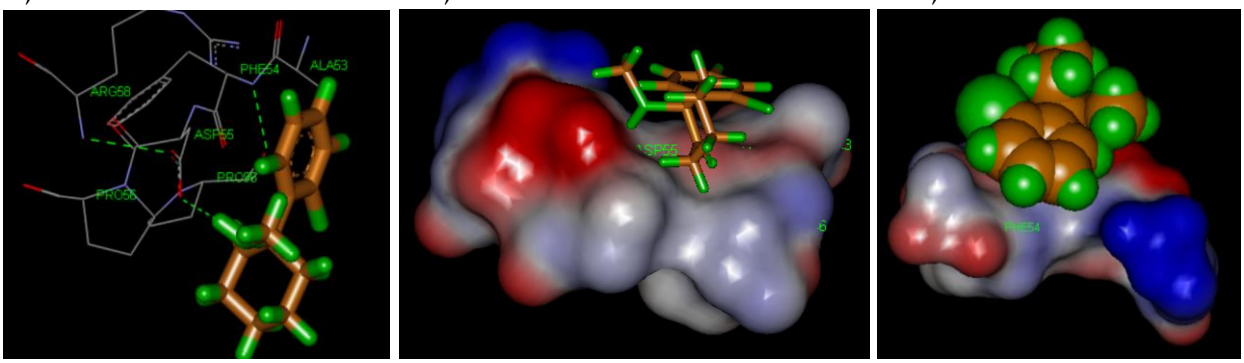

Figure 6: The best binding mode of **RKE** with the active site of the pLGICs receptor. a) The H-bond interactions between **RKE** and the binding site of pLGIC. b) The docked pose of 3D structure (stick model) of in pLGIC pocket. c) The docked pose of 3D CPK conformation in pLGIC pocket.

Compounds **19S, 20R, 21R** and **22R** have the lowest binding energies and consequently the lowest inhibition constants in comparison to **JC9** and **RKE**. As described in figure 7 the compound **19S** donates three hydrogen bonds via the three polar hydrogen atoms of the primary and secondary amines with oxygen atoms of Tyr66, Glu67 and Ile92, while the non-polar part of cyclohexanone and aromatic ring form hydrophobic attractions with non-polar residues, Pro68, and the branched chain of Val89, Val90 and Ile92.

a) b) c)

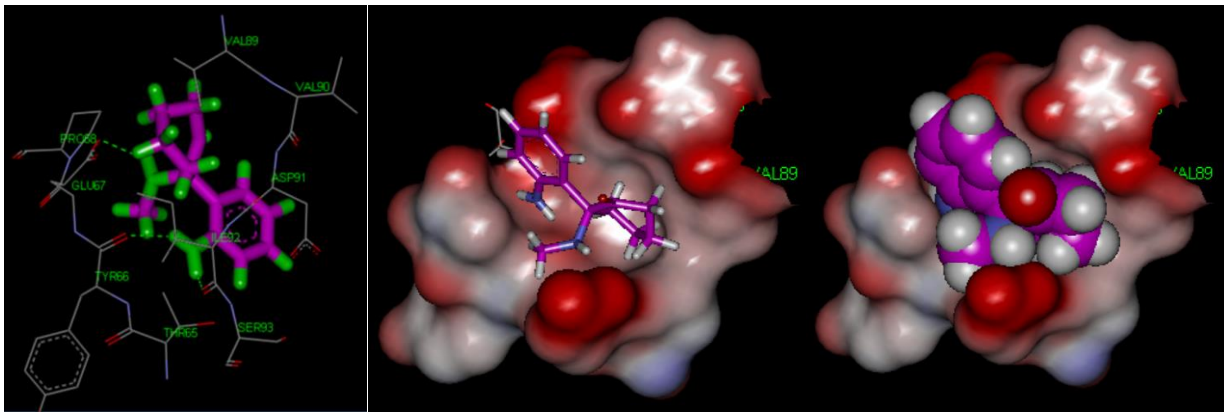

Figure 7: The best binding mode of **19S** with the active site of the pLGICs receptor. a) The H-bond interactions between **19S** and the binding site of pLGIC. b) The docked pose of 3D structure (stick model) in pLGIC pocket. c) The docked pose of 3D CPK conformation in pLGIC pocket.

The best binding mode of the compound **20R** with the active site of the pLGICs receptor is shown in figure 8.

a) b) c)

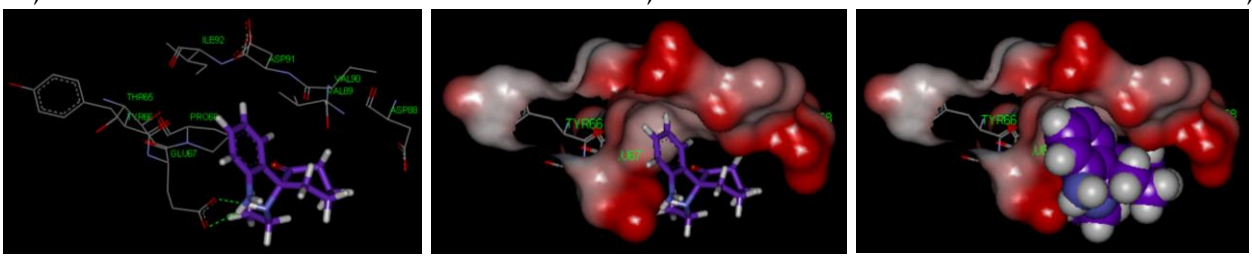

Figure 8: The best binding mode of **20R** with the active site of the pLGICs receptor. a) The H-bond interactions between **20R** and the binding site of pLGIC. b) The docked pose of 3D structure (stick model) in pLGIC pocket. c) The docked pose of 3D CPK conformation in pLGIC pocket.

Compounds **21R** and **22R** have the same mode of binding with the active site. Each molecule can form five hydrogen bonds by accepting one hydrogen bond from N atom of Ile92 and donating four hydrogen bonds to Tyr66, Ile92 and two oxygen atoms Glu67 carboxylate as shown in figure 9 for compound **21R** and figure 10 for compound **22R**. The interaction of the most potent compounds, **19S**, **20R**, **21R** and **22R** with the active site indicates the possible localization of these compounds in the same manner used by the standard ligand as shown in figure 11.

a) b) c)

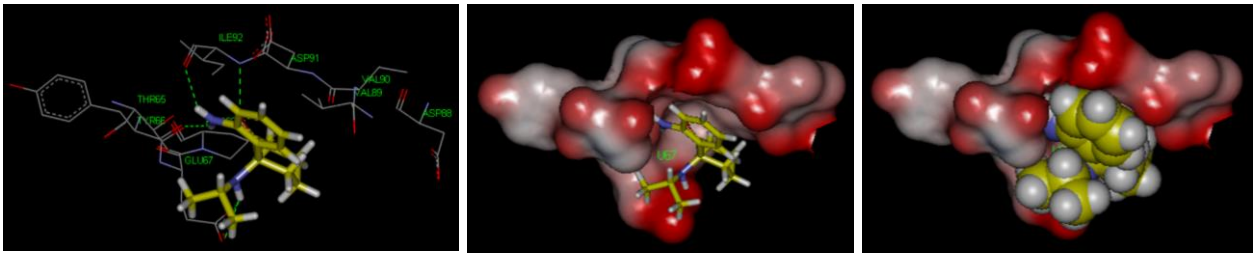

Figure 9: The best binding mode of **21R** with the active site of the pLGICs receptor. a) The H-bond interactions between **21R** and the binding site of pLGIC. b) The docked pose of 3D stick conformation in pLGIC pocket. c) The docked pose of 3D CPK conformation in pLGIC pocket.

a) b) c)

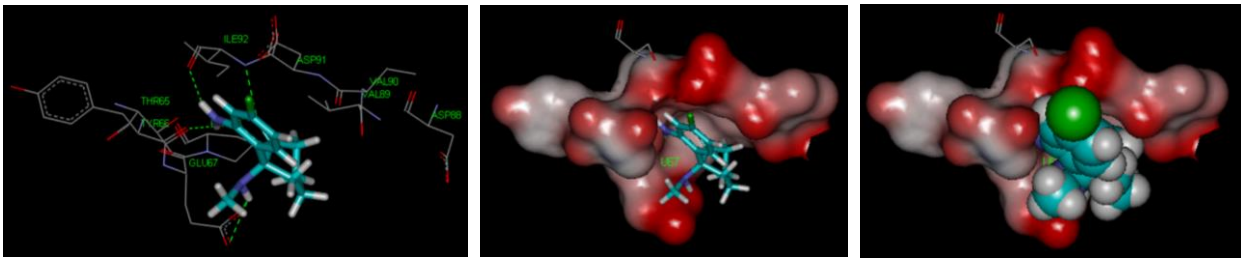

Figure 10: The best binding mode of **22R** with the active site of the pLGICs receptor. a) The H-bond interactions between **22R** and the binding site of pLGIC. b) The docked pose of 3D stick conformation in pLGIC pocket. c) The docked pose of 3D CPK conformation in pLGIC pocket.

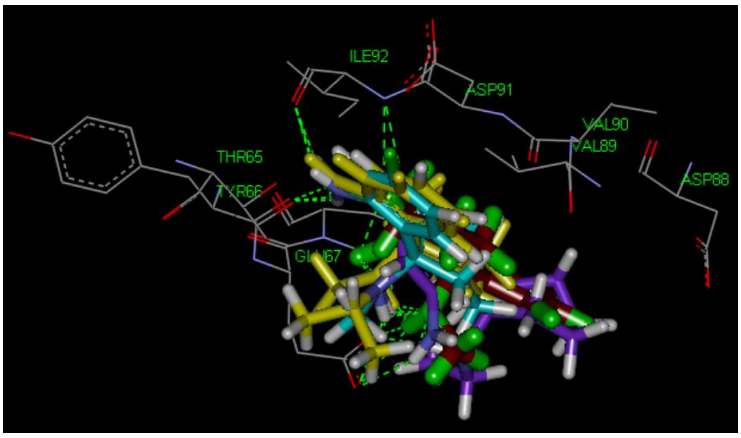

Figure 11: The binding mode of compounds **19S**, **20R, 21R, 22R** and **JC9** in the active site of pLGIC receptor.

3.2. Drug-likeness

The physicochemical properties of all the designed molecules were calculated using online Swiss ADME tool and the results were listed in table 2, while drug-likeness results in table 3. From table 2, it is observed that the molecular weight values of the designed compounds ranged from 217.31 to 310.23 (<500), the number of hydrogen bond donor (HBD) ranged from 1 to 2 (< 5), the number of hydrogen bond acceptor (HBA) ranged from 2 to 4 (< 10) and the value of log (octanol/water) partition coefficient (log P) ranged from 1.49 to 3.41 (< 5)[33]. This means that all designed molecules obey to the Lipinski Rules of Five, with 0 violation as illustrated in table 3. These result indicate that all molecules have good oral absorption and permeation.

In addition, the number of rotatable bonds ranged from 2 to 4 (< 10) and total polar surface area TPSA ranged from 29.10 to 74.29 (<140 Å^2), this means that all designed molecules obey to the Veber rules with 0 violation [34]. Moreover, the molar refractivity ranged from 60.98 to 79.46 (40-130), WLOGP ranged from 1.73 to 3.68 (-0.4-5.6), 180≤MW≤480 and 20≤atoms≤70, this means that all molecules obey to the Ghose rules with 0 violation [35]. Furthermore, all designed molecules obey Egan rule (WLOGP≤5.88 and TPSA≤131.6) with 0 violation [36]. The aqueous solubility of all designed compounds was predicted form the LogS (Ali) values (implemented from Ali J. *et. Al.* in 2012) range -3.39 to -1.61, indicating that all compounds are predicted to be soluble [37].

Table 2: The predicted physiochemical properties

Cpds	Formula	MW	nRot.B	HBD	HBA	MR	TPSA °A^2	MLog P	WLOGP	Log S (Ali)
1S, 1R	C13H16FNO	221.27	2	1	3	60.98	29.10	2.33	2.70	−2.27
2S, 2R	C13H16BrNO	282.18	2	1	2	68.72	29.10	2.59	2.90	−2.49
3S, 3R	C13H17NO2	219.28	2	2	3	63.04	49.33	1.31	1.84	−1.83
4S, 4R	C13H16N2O3	248.28	3	1	4	69.84	74.92	0.75	2.57	−2.56
5S, 5R	C14H19NO	217.31	2	1	2	65.99	29.10	2.19	2.44	−2.15
6S, 6R	C13H16ClNO	237.73	2	1	2	66.03	29.10	2.46	2.79	−2.42
7S, 7R	C14H18ClNO	251.75	3	1	2	70.84	29.10	2.71	3.18	−2.81
8S, 8R	C15H20ClNO	265.78	3	1	2	75.64	29.10	2.96	3.57	−3.25
9S, 9R	C13H16ClNO	237.73	2	1	2	66.03	29.10	2.46	2.79	−2.42
10S, 10R	C13H16BrNO	282.18	2	1	2	68.72	29.10	2.59	2.90	−2.49
11S, 11R	C14H18BrNO	−2.49	3	1	2	73.53	29.10	2.84	2.84	−2.87
12S, 12R	C15H20BrNO	310.23	3	1	2	78.33	29.10	3.09	3.68	−3.32
13S, 13R	C14H19NO2	233.31	3	2	3	67.85	49.33	1.58	2.32	−2.21
14S, 14R	C15H21NO2	247.33	3	2	3	72.66	49.33	1.83	2.62	−2.66
15S, 15R	C14H18N2O3	262.30	4	1	4	74.65	74.92	1.01	2.96	−2.94
16S, 16R	C15H20N2O3	276.33	4	1	4	79.46	74.92	1.27	3.35	−3.39
17S, 17R	C12H15ClN2O	238.71	2	1	3	63.83	41.99	1.31	2.18	−2.33
18S, 18R	C12H15BrN2O	283.16	2	1	3	66.52	41.99	1.45	2.29	−2.39
19S, 19R	C13H18N2O	218.29	2	2	2	65.43	55.12	1.31	1.73	−1.61
20S, 20R	C14H20N2O	232.32	3	2	2	70.23	55.12	1.58	2.12	−2.00
21S, 21R	C15H22N2O	246.35	3	2	2	75.04	55.12	1.83	2.50	−2.44
22S, 22R	C13H17ClN2O	252.74	2	2	2	70.44	55.12	1.85	2.38	−2.27
JC9 & RKE	C13H16ClNO	237.73	2	2	1	66.03	29.10	2.46	2.79	−2.42

MW− Molecular weight, nRotB− No. of rotatable bonds, nHBA− No. of hydrogen bond acceptor(s), nHBD− No. of hydrogen bond donor(s), MR− Molar refractivity, TPSA−Total polar surface area, MLogP− (Partitioning coefficient calculated by the Moriguchi I. *et al.*) WlogP (Partitioning coefficient calculated by the Wildman *et al.*), Stand−standard, LogS (Ali j *et al*).

The predicted bioavailability scores of all designed compounds were 0.55, which implied that they had 55% probability of rat bioavailability (higher than 10%), thus all these compounds are expected to have good oral bioavailability [38].

Table 3: The drug-likeness of designed compounds

Cpd	Lipinski's rule of five MW<500Da MLogP<5 HBD< 5 HBA<10	Ghose 160≤MW≤480 −0.4≤WLOGP ≤5.6 40≤MR≤130 20≤atoms≤70	Veber nRot.B ≤10 TPSA≤140	Egan WLOGP≤5.88 TPSA≤131.6	Bioavailability Score
1S &1R	Yes; 0 violation	Yes; 0 violation	Yes; 0 violation	Yes; 0 violation	0.55
2S &2R	Yes; 0 violation	Yes; 0 violation	Yes; 0 violation	Yes; 0 violation	0.55
3S &3R	Yes; 0 violation	Yes; 0 violation	Yes; 0 violation	Yes; 0 violation	0.55
4S &4R	Yes; 0 violation	Yes; 0 violation	Yes; 0 violation	Yes; 0 violation	0.55
5S &5R	Yes; 0 violation	Yes; 0 violation	Yes; 0 violation	Yes; 0 violation	0.55
6S &6R	Yes; 0 violation	Yes; 0 violation	Yes; 0 violation	Yes; 0 violation	0.55
7S &7R	Yes; 0 violation	Yes; 0 violation	Yes; 0 violation	Yes; 0 violation	0.55
8S &8R	Yes; 0 violation	Yes; 0 violation	Yes; 0 violation	Yes; 0 violation	0.55
9S &9R	Yes; 0 violation	Yes; 0 violation	Yes; 0 violation	Yes; 0 violation	0.55
10S &10R	Yes; 0 violation	Yes; 0 violation	Yes; 0 violation	Yes; 0 violation	0.55
11S &11R	Yes; 0 violation	Yes; 0 violation	Yes; 0 violation	Yes; 0 violation	0.55
12S &12R	Yes; 0 violation	Yes; 0 violation	Yes; 0 violation	Yes; 0 violation	0.55
13S &13R	Yes; 0 violation	Yes; 0 violation	Yes; 0 violation	Yes; 0 violation	0.55
14S &14R	Yes; 0 violation	Yes; 0 violation	Yes; 0 violation	Yes; 0 violation	0.55
15S &15R	Yes; 0 violation	Yes; 0 violation	Yes; 0 violation	Yes; 0 violation	0.55
16S &16R	Yes; 0 violation	Yes; 0 violation	Yes; 0 violation	Yes; 0 violation	0.55
17S &17R	Yes; 0 violation	Yes; 0 violation	Yes; 0 violation	Yes; 0 violation	0.55
18S &18R	Yes; 0 violation	Yes; 0 violation	Yes; 0 violation	Yes; 0 violation	0.55
19S &19R	Yes; 0 violation	Yes; 0 violation	Yes; 0 violation	Yes; 0 violation	0.55
20S &20R	Yes; 0 violation	Yes; 0 violation	Yes; 0 violation	Yes; 0 violation	0.55
21S &21R	Yes; 0 violation	Yes; 0 violation	Yes; 0 violation	Yes; 0 violation	0.55
22S &22R	Yes; 0 violation	Yes; 0 violation	Yes; 0 violation	Yes; 0 violation	0.55
JC9 & RKE	Yes; 0 violation	Yes; 0 violation	Yes; 0 violation	Yes; 0 violation	0.55

3.3. Bioactivity score prediction

The predicted bioactivity scores, for all the designed molecules calculated by Molinspiration web. server, were listed in table 4. As shown in table 4, all molecules have good ion channel modulator activities with bioactivity scores from 0.02 to 0.86, except molecules **11S** and **11R**, which are moderately active with bioactive score −

0.04. Moreover, (9) of designed compounds (**3, 13, 14, 17, 18, 19, 20, 21** and **22**), whether the S isomers or R isomers are predicted to be good enzyme inhibitory. (A bioactivity score values > 0.00 good biological activity, values −0.50 to 0.00 moderately active, and values < −0.50 biologically inactive) [39].

Table 4: Bioactivity score prediction of designed compounds

Cpds	GPCR Ligand	Ion channel modulator	Kinase Inhibitor	Nuclear receptor Ligand	Protease Inhibitor	Enzyme Inhibitor
1S &1R	−0.50	0.18	−0.93	−0.66	−0.46	−012
2S &2R	−0.61	0.14	−1.00	−0.77	−0.58	−0.14
3S &3R	−0.52	0.34	−0.97	−0.54	−0.38	0.07
4S &4R	−0.45	0.30	−0.92	−0.46	−0.34	−0.01
5S &5R	−0.44	0.26	−1.05	−0.73	−0.65	−0.12
6S &6R	−0.41	0.31	−0.95	−0.68	−0.39	−0.09
7S &7R	−0.41	0.08	−1.04	−0.69	−0.41	−0.21
8S &8R	−0.34	0.13	−0.91	−0.55	−0.39	−0.15
9S &9R	−0.42	0.30	−0.93	−0.67	−0.39	−0.09
10S &10R	−0.58	0.19	−0.97	−0.81	−0.50	−0.15
11S &11R	−0.48	−0.04	−1.02	−0.74	−0.44	−0.17
12S &12R	−0.41	0.02	−0.90	−0.60	−0.42	−0.11
13S &13R	−0.39	0.14	−0.99	−0.53	−0.26	0.04
14S &14R	−0.32	0.19	−0.86	−0.39	−0.25	0.08
15S &15R	−0.34	0.11	−0.94	−0.46	−0.23	−0.04
16S &16R	−0.29	0.15	−0.84	−0.35	−0.23	−0.01
17S &17R	−0.30	0.60	−0.72	−0.61	−0.39	0.09
18S &18R	−0.25	0.86	−0.51	−0.47	−0.22	0.40
19S &19R	−0.32	0.47	−0.73	−0.65	−0.19	0.25
20S &20R	−0.20	0.27	−0.76	−0.63	−0.07	0.20
21S &21R	−0.15	0.31	−0.65	−0.49	−0.08	0.24
22S &22R	−0.25	0.46	−0.64	−0.57	−0.21	0.20
JC9 & **RKE**	−0.54	0.27	−1.02	−0.72	−0.54	−0.19

GPCR− G−protein coupled receptor

4. Conclusion

From the molecular docking study, drug−likeness, bioactivity score prediction and ADME screening, it was confirmed that the (16) molecules, (12) of the (S)− isomers of the designed molecules, (**3, 4, 5, 7, 8, 9, 12, 18, 19,20, 21 and 22**) and (4) of the (R)−isomers (**12, 20, 21, 22**) are predicted to have more anesthetic activities than the two enantiomers S and R−ketamine molecules. The molecules **8S, 19S**, **22S**, **20R**, **21R**, and **22R** are predicted to be the most potent anesthesia drugs, with good oral bioavailability scores and good modulators of ion channels. This is explained by their higher affinities to target receptor and lower binding energy ranging from −6.23

Kcal/mol to −6.6 Kcal/mol, than S and R−ketamine isomers. Moreover, these compounds have lower inhibition constants ranging from 27.11 M to 14.64 M, which are much lower than the inhibition constants of S and R−ketamine isomers. It is concluded that these compounds mediate their anesthetic activities by regulating the ion channels in central nervous system and lower doses of these compounds are required to mediate their anesthetic activities.

Acknowledgement:

Authors would like to thank D. slash ben saber who passed away for his endless helps regard AutoDock software training

References:

[1] James E. Svenson MD, MS, Michael K. Abernathy MD. Ketamine for prehospital use: new look at an old drug. American Journal of Emergency Medicine 2007; 25: 977 – 980

[2] Le Daré B, Pelletier R, Morel I, Gicquel T. History of Ketamine: an ancient molecule that is still popular today. Annales Pharmaceutiques Françaises 2022; 80(1):1−8.

[3] Johnstone M, Evans V, Baigel S. Sernyl (CI−395) in clinical anaesthesia. British Journal of Anaesthesia. 1959; 31:433−439.

[4] Lear E, Suntay R, Pallin IM and Chiron AE. Cyclohexamine (CI−400). A new intravenous agent. Anesthesiology 1959; 20:330−335.

[5] Li L, Vlisides PE: Ketamine: 50 years of modulating the mind. Frontiers in Human Neuroscience. 2016; 10(612):1−15.

[6] Domino EF. Taming the ketamine tiger. 1965. Anesthesiology 2010; 113:678−684.

[7] Zhornitsky S, Oliva H, Jayne L, Allsop A, Kaye A, Potenza M and Angarita G. Changes in synaptic markers after administration of ketamine or psychedelics: a systematic scoping review. Frontiers in Psychiatry. 2023;14: 1197890.

[8] Marion V, Céline L, Bruno P, Gisèle P. Assessment of Initial Depressive State and Pain Relief with Ketamine in Patients with Chronic Refractory Pain. Journal of the American Medical Association. 2023;6(5):1−13.

[9] Abdullah SB, Deipthan P, Mohammed A, Cassie J, Mohammed A. Evaluating the Safety and Efficacy of Ketamine as a Bronchodilator in Pediatric Patients with Acute Asthma Exacerbation: A Review. Cureus 2023;14:(6):1−9.

[10] Zhang J, Ma1 Q,2, Li W, Li X and Chen X. S−Ketamine attenuates inflammatory effect and
modulates the immune response in patients undergoing modified radical mastectomy: A prospective randomized controlled trial. Frontiers in Pharmacology. 2023; 10.3389: 1−10.

[11] Ilkjaer S, petersen KL, brennum J, wernberg M AND dahl JB. Effect of systemic N−methyl−D−aspartate receptor antagonist (ketamine) on primary and secondary hyperalgesia in humans. British Journal of Anaesthesia 1996; 76: 829−834.

[12] Wei Y, Chang L, Hashimoto K. A historical review of antidepressant effects of ketamine and its enantiomers. Pharmacology, Biochemistry and Behavior 2020; 190:1−9

[13] Fung EL, Yam KM, Yau ML. Ketamine use for super−refractory status epilepticus in children. Hong Kong Medical Journal. 2020; 26:549−550

[14] Adnan TB, Michael LS, Christopher S, Laura PJ, Wendy LW, Diana ML, Charles MG,

Volkan T, Parthak P, Umesh D, Michiaki I, Robert DB, Kanwaljeet JS. Ketamine as a neuroprotective and anti-inflammatory agent in children undergoing surgery on cardiopulmonary bypass: A pilot randomized, double-blind, placebo-controlled trial. Pediatric Critical Care Medicine. 2012; 3:328–337.

[15] White PF, Schuttler J, Shafer J, Stanski DR, Horai Y. and Trevor AJ. Comparative pharmacology of the ketamine isomers. British Journal of Anaesthesia. 1985; 57: 197–203

[16] Charles FZ, Yukitoshi I, and Steven M. Ketamine: NMDA Receptors and Beyond. The Journal of Neuroscience 2016; 36(44):11158–11164

[17] Pan J, Chen Q, Willenbring D, Mowrey D, Kong X, Cohen A, Christopher BD, Xu Y and Tang P. Structure of the Pentameric Ligand-Gated Ion Channel GLIC Bound with Anesthetic Ketamine. Cell press 2012; 20: 1463–1469.

[18] Thompson AJ, Lester HA, Lummis SC. The structural basis of function in Cys-loop receptors. Quarterly Reviews of Biophysics. 2010; 43: 449–499.

[19] Jansen M, Bali M, Akabas MH. Modular design of Cys-loop ligand-gated ion channels: functional 5-HT3 and GABA rho1 receptors lacking the large cytoplasmic M3M4 loop. Journal of General Physiology. 2008; 131: 137–146.

[20] Bocquet N, Nury H, Baaden M, Poupon C, Changeux JP, Changeux JP, Delarue M and Corringer PJ. X-ray structure of a pentameric ligand-gated ion channel in an apparently open conformation. Nature 2009; 457: 111–114.

[21] Unwin N. Refined Structure of the Nicotinic Acetylcholine Receptor at 4A° Resolution. Journal of Molecular Biology. 2005;346: 967–989.

[22] Costa CJ and Baenzige JE. Gating of Pentameric Ligand-Gated Ion Channels: Structural Insights and Ambiguities. Cell press 2013;21(8): 1271–1283.

[23] Douglas B Kitchen, Helene Decornez, John R Furr, Jurgen Bajorath. Docking and scoring in virtual screening for drug discovery: methods and applications. Nature Reviews Drug Discovery. 2004;3: 935–949.

[24] Morris GM, Huey R, Lindstrom W, Sanner MF, Belew RK, Goodsell DS, Olson AJ. Auto-Dock4 and AutoDockTools4: automated docking with selective receptor flexibility. Journal of Computational Chemistry. 2009; 30(16): 2785–2791.

[25] Denish P, Miloni B and Chintan S. A review on computational chemistry software for drug designing and discovery. World Journal of Pharmaceutical Research. 2022; 11(12): 830–851.

[26] Daina A, Michielin O, Zoete V. SwissADME: a free web tool to evaluate pharmacokinetics, drug-likeness and medicinal chemistry friendliness of small molecules. Scientific Reports. 2017; 7(42717): 1–13.

[27] Syed M, Danish R, Shazi S and Haneef M. A simple click by click protocol to perform docking: autodock 4.2 made easy for non-bioinformaticians. Experimental and Clinical Sciences Journal 2013; 12:831–857.

[28] Moriguchi I, Hirono S, Liu Q, Nakagome I, Matsushita Y. Simple method of calculating octanol/water partition coefficient. Chemical and Pharmaceutical Bulletin. 1992; 40(1):127–130.

[29] Wildman SA and Crippen GM. Prediction of physicochemical parameters by atomic contributions. Journal of chemical information and computer sciences. 1999; 39: 868–873.

[30] Lipinski CA, Lombardo F, Dominy BW and Feeney PJ. Experimental and computational approaches to estimate solubility and permeability in drug discovery and development settings. Advanced Drug Delivery Reviews. 2001; 46, 3–26.

[31] Veber, DF, Johnson SR, Cheng, HY, Smith BR, Ward, KW and Kopple KD. Molecular properties that influence the oral bioavailability of drug candidates. Journal of Medicinal Chemistry. 2002;45: 2615–2623.

[32] Egan WJ, Merz KM, and Baldwin JJ. Prediction of drug absorption using multivariate statistics. Journal of Medicinal Chemistry. 2000, 43: 3867–3877.

[33] Violeta I, Miroslav R, Biljana Ar and Aleksandra P. Lipinski's rule of five, famous extensions and famous exceptions. Chemia Naissensis. 2020; 3 (1): 171–177

[34] Brito MA. Pharmacokinetic study with computational tools in the medicinal chemistry course. Brazilian Journal of Pharmaceutical Sciences. 2011; 47(4): 797–805.

[35] Sebastjan K, Marko J, and Urban B. Comparative Analyses of Medicinal Chemistry and Cheminformatics Filters with Accessible Implementation in Konstanz Information Miner (KNIME). International Journal of Molecular Sciences. 2022; 23(10): 5727.

[36] Pathania S and Singh PK. Analyzing FDA-approved drugs for compliance of pharmacokinetic principles: should there be a critical screening parameter in drug designing protocols?. Expert Opinion on Drug Metabolism & Toxicology. 2021; 17(4): 351–354.

[37] Ali J, Camilleri P, Brown MB, Hutt AJ, and Kirton SB. In silico prediction of aqueous solubility using simple QSPR models: The importance of phenol and phenol-like moieties. Journal of Chemical Information and Modeling. 2012; 52: 2950–2957.

[38] Zhu J, Wang J, Yuc H, Li Y,1 and Hou T. Recent developments of in silico predictions of oral bioavailability. Combinatorial Chemistry & High Throughput Screening. 2011; 14(5): 1–13

[39] Tahmeena K, Shalini D, Rumana A, Saman R, Iqbal A, Seema J and Abdul Rahman K. Molecular docking, PASS analysis, bioactivity score prediction, synthesis, characterization and biological activity evaluation of a functionalized 2-butanone thiosemicarbazone ligand and its complexes. Journal of Chemical Biology. 2017; 10:91–104.